Half-Duplex Base Station with Adaptive Scheduling of the in-Band Uplink-Receptions and Downlink-Transmissions

Mohsen Mohammadkhani Razlighi and Nikola Zlatanov

Abstract

In this paper, we propose a novel reception/transmission scheme for half-duplex base stations (BSs). In particular, we propose a half-duplex BS that employes in-band uplink-receptions from user 1 and downlink-transmissions to user 2, which occur in different time slots. Furthermore, we propose optimal adaptive scheduling of the in-band uplink-receptions and downlink-transmissions of the BS such that the uplink-downlink rate/throughput region is maximized and the outage probabilities of the uplink and downlink channels are minimized. Practically, this results in selecting whether in a given time slot the BS should receive from user 1 or transmit to user 2 based on the qualities of the in-band uplink-reception and downlink-transmission channels. Compared to the performance achieved with a conventional full-duplex division (FDD) base station, two main gains can be highlighted: 1) Increased uplink-downlink rate/throughput region; 2) Doubling of the diversity gain of both the uplink and downlink channels.

I. Introduction

There are two conventional modes of operation for a half-duplex[1] base station (BS), a time-division duplex (TDD) mode and a frequency-division duplex (FDD) mode, see [1]. A BS operating in the FDD mode, also known as a FDD-BS, does not perform in-band receptions and transmissions, i.e., the receptions and the transmissions of the FDD-BS are separated in different frequency bands. On the other hand, a BS operating in the TDD mode, also known as a TDD-BS, performs in-band uplink-receptions and downlink-transmissions, which are separated in different time slots, i.e., in a given time slot either an uplink-reception or a downlink-transmission can

M. M. Razlighi N. Zlatanov are with the Department of Electrical and Computer Systems Engineering, Monash University, Melbourne, VIC 3800, Australia (e-mails: mohsen.mohammadkhanirazlighi@monash.edu and nikola.zlatanov@monash.edu.)

[1]A half-duplex base station cannot simultaneously transmit and receive in the same frequency band due to self-interference.

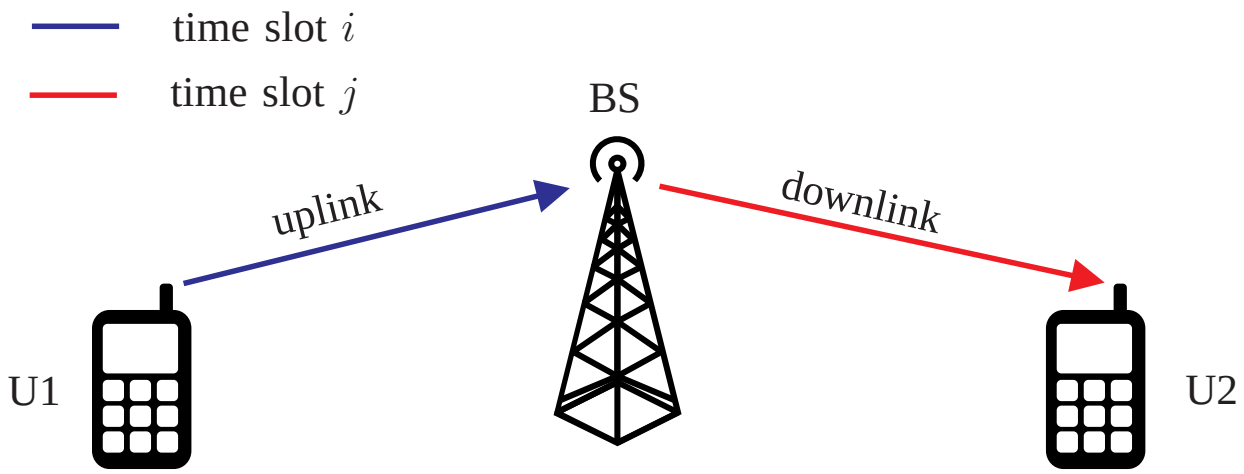

Fig. 1. System model comprised of a half-duplex BS, user 1 (U1) and user 2 (U2), where $i \neq j$.

occur. However, the in-band uplink-receptions and downlink-transmissions of the TDD-BS are from/to a single user. As a result, the in-band uplink and downlink channels experience identical fading in a given time slot. Hence, if the uplink channel is weak in a given time slot, then the downlink channel would also be weak, and vice versa. If we could devise a scheme where the in-band uplink-reception and downlink-transmission channels would experience independent fadings, then a diversity gain could be achieved by selecting the stronger of the uplink and downlink channel for transmission in a given time slot.

To obtain in-band uplink and downlink channels that experience independent fading, we propose a BS which employs in-band uplink-receptions and downlink-transmissions from/to two different users, respectively. More precisely, we propose the BS to receive from user 1 (U1) in the uplink and to transmit to user 2 (U2) in the downlink in the same frequency band but in different time slots, cf. Fig. 1. Next, we propose to use adaptive scheduling of the in-band uplink-receptions and downlink-transmissions of the BS based on the qualities of the in-band uplink and downlink channels such that the uplink-downlink rate/throughput region is maximized. In this way, we obtain a diversity gain which is not present in conventional schemes, such as FDD-BS and TDD-BS.

The simplest scheduling of the in-band uplink-receptions and downlink-transmissions proposed in this paper operates in the following manner. In the beginning of a given time slot, the BS compares whether the in-band uplink-reception or the downlink-transmission channel is stronger, and selects that channel for transmission in the given time slot. In particular, if the uplink-reception channel is stronger than the downlink-transmission channel, then, in the given time

slot, U1 performs an uplink transmission to the BS (i.e., the BS receives), otherwise, the BS performs a downlink transmission to U2 (i.e., the BS transmits). Our numerical results show that the proposed scheduling scheme of the in-band uplink-receptions and downlink-transmissions of a BS provides significant performance gains compared to the performance of a FDD-BS. In particular, the numerical results show an increase of the rate/throughput region, around 3 dB power gain of the uplink-downlink sum rate, and doubling of the diversity gain on both the uplink-reception and downlink-transmission channels.

To the best of our knowledge, although the proposed concept is very simple and effective, it has not been reported in the literature, yet. Hence, this is the first proposed scheme for a half-duplex BS to employ in-band uplink-receptions and downlink-transmissions from/to two users, respectively, where the in-band uplink-receptions and downlink-transmissions are scheduled such that the uplink-downlink rate/throughput region is maximized.

In the literature, there are opportunistic schedulers which take advantage of the channel state information (CSI) at the user and BS sides in order to guarantee a certain level of quality of service (QoS) or increased data rates, see [2]–[14]. However, these works consider the conventional FDD- and/or TDD-BSs, and do not propose a scheme similar to the one proposed in this paper. On the other hand, lately, there has been an increased interest in full-duplex BSs which can simultaneously receive and transmit on the same frequency band, see [15]–[23]. In [15]–[23], there are cases for which the full-duplex BS switches to the half-duplex mode. However, even for those cases, the proposed schemes are not similar to the schemes proposed in this paper.

Remark 1: There have been proposals recently for decoupling the uplink and downlink transmissions at the users, see [24]. Hence, instead of coupling the uplink and downlink transmissions of a user to/from a single BS, to have an uplink and downlink transmissions to/from two BSs, respectively, cf. Fig. 2. We note that such a system model, i.e., single user with uplink-transmissions and downlink-receptions to/from two BSs, respectively, is almost identical to the considered system model in this paper, i.e., BS that employs uplink-receptions and downlink-transmission from/to two users, respectively. As a result, the protocols proposed in this paper for the system model with one BS and two users, cf. Fig. 1, are directly applicable to the system model with one user employing decoupled *in-band* uplink-transmissions and downlink-receptions to/from two BSs, cf. Fig. 2. Using the proposed protocols, the user can adaptively select whether

to have an *in-band* uplink-transmission to BS2 or a downlink-reception from BS1 in a given time slot, and thereby achieve significant performance gains compared to previous schemes where a user employs coupled uplink-downlink transmissions to/from a single BS or a user employs decoupled but *out-of-band* uplink-transmissions to BS2 and downlink-receptions from BS1. In particular, increased uplink-downlink rate/throughput region and doubling of the diversity gain on both the uplink and downlink channels can be observed. Hence, the contributions of this paper are two-fold since the proposed schemes improve the performance of the system models in both Fig. 1 and Fig. 2. Moreover, an implicit consequence of the results in this paper is that both the BSs and the users in a cellular network should employ adaptive scheduling of the *in-band* receptions and transmissions from different users and BSs, respectively, as proposed in this paper, in order to harness the available diversity gains of the cellular network.

The rest of this paper is organized as follows. In Section II, we present the system and channel models. In Section III, we formulate a general scheme for adaptive scheduling of the in-band uplink-receptions and downlink-transmissions of a BS. In Section IV, we propose specific schemes for continuous-rate transmission with adaptive- and fixed-power allocation, and derive the corresponding uplink-downlink rate regions. The uplink-downlink throughput region for transmission with predefined discrete transmission rates is derived in Section V. In Section VI, we propose two practical schemes for achieving a desired level of fairness among the uplink and downlink rates. Simulation and numerical results are provided in Section VII, and the conclusions are drawn in Section VIII.

II. System and Channel Models

We consider a three-node system model comprised of a BS operating in the half-duplex mode, an uplink user, U1, and a downlink user, U2, as illustrated in Fig. 1. The BS receives information from U1 in the uplink and transmits information to U2 in the downlink in the same frequency band. Since the BS operates in the half-duplex mode, the in-band uplink-receptions and downlink-transmissions do not occur simultaneously. Instead, in a given time slot, either an uplink-reception or a downlink-transmission occurs at the BS, cf. Fig. 1.

A. Channel Model

We assume that the U1-BS and BS-U2 links are complex-valued additive white Gaussian noise (AWGN) channels impaired by slow fading. We assume that the transmission time is divided

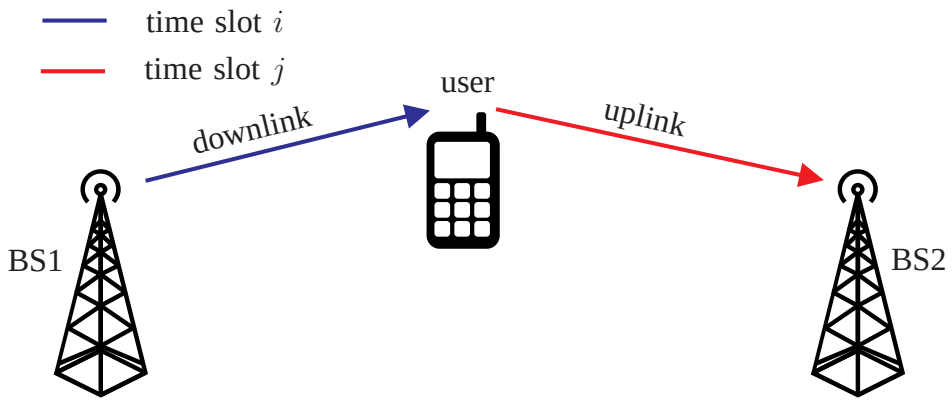

Fig. 2. System model comprised of a user with decoupled in-band uplink-transmissions to base station 2 (BS2) and downlink-receptions from base station 1 (BS1), where $i \neq j$.

into $N \to \infty$ time slots. Furthermore, we assume that the fading is constant during one time slot and changes from one time slot to the next. In time slot i, let the complex-valued fading gains of U1-BS and BS-U2 channels be denoted by $h_1(i)$ and $h_B(i)$, respectively. Moreover, let the variances of the complex-valued AWGNs at BS and U2 be denoted by σ_B^2 and σ_2^2, respectively. For convenience, we define normalized magnitude-squared fading gains of the U1-BS and BS-U2 channels as $\gamma_1(i) = |h_1(i)|^2/\sigma_B^2$ and $\gamma_B(i) = |h_B(i)|^2/\sigma_2^2$, respectively. Furthermore, let the transmit powers of U1 and BS in time slot i be denoted by $P_1(i)$ and $P_B(i)$, respectively. As a result, the capacities of the U1-BS and BS-U2 channels in time slot i, denoted by $C_1(i)$ and $C_B(i)$, respectively, are obtained as

$$C_1(i) = \log_2(1 + P_1(i)\gamma_1(i)), \tag{1}$$

$$C_B(i) = \log_2(1 + P_B(i)\gamma_B(i)). \tag{2}$$

In time slot i, we assume that U1 and BS transmit codewords encoded with a capacity achieving code, i.e., codewords comprised of $n \to \infty$ symbols that are generated independently from complex-valued zero-mean Gaussian distributions with variances $P_1(i)$ and $P_B(i)$, respectively. The data rates of the codewords transmitted by U1 and BS in time slot i, denoted by $R_1(i)$ and $R_B(i)$, respectively, will depend on the specific scheme and will be defined later on in the paper.

III. General Scheme for Adaptive Scheduling of the in-Band Uplink-Receptions and Downlink-Transmissions of a Base Station

In this section, we formulate a general communication scheme for adaptive scheduling of the in-band uplink-receptions and downlink-transmissions of a half-duplex BS.

A. Problem Formulation

In a given time slot, depending on whether the BS receives from U1 in the uplink or transmits to U2 in the downlink, the considered three-node network, shown in Fig. 1, can be in one of the following three states

- *State 0:* U1 and BS are both silent.
- *State 1:* U1 transmits to BS and BS is silent.
- *State 2:* BS transmits to U2 and U1 is silent.

In order to model the three network states for time slot i, we define two binary variables $q_1(i)$ and $q_B(i)$, as

$$q_1(i) = \begin{cases} 1 & \text{if U1 transmits to BS and BS is silent in time slot } i \\ 0 & \text{otherwise,} \end{cases} \tag{3}$$

$$q_B(i) = \begin{cases} 1 & \text{if BS transmits to U2 and U1 is silent in time slot } i \\ 0 & \text{otherwise.} \end{cases} \tag{4}$$

Since the considered network can by in one and only one of the three states in time slot i, the following has to hold

$$q_1(i) + q_B(i) \in \{0, 1\}, \tag{5}$$

where if $q_1(i) + q_B(i) = 0$ holds, it means that the network is in State 0, i.e., U1 and BS are both silent in time slot i. Condition (5) results from the half-duplex constraint of the BS, i.e., the BS can either transmit or receive in a given time slot in the same frequency band.

Our task in this paper is to find the maximum uplink-downlink rate/throughput region by selecting the optimal values of $R_1(i)$, $R_B(i)$, $q_1(i)$, $q_B(i)$, $P_1(i)$, and $P_B(i)$, for $i = 1, ...N$, where $N \to \infty$, which are the only possible variables with a degree of freedom. To this end,

we define the following auxiliary state-selection scheme for time slot i

$$\begin{aligned}
&\bullet\ [q_1(i)=1 \text{ and } q_B(i)=0] \text{ if } [\Lambda_1(i)\geq\Lambda_B(i) \text{ and } \Lambda_1(i)>0],\\
&\bullet\ [q_1(i)=0 \text{ and } q_B(i)=1] \text{ if } [\Lambda_B(i)>\Lambda_1(i) \text{ and } \Lambda_B(i)>0],\\
&\bullet\ [q_1(i)=0 \text{ and } q_B(i)=0] \text{ if } [\Lambda_1(i)\leq 0 \text{ and } \Lambda_B(i)\leq 0],
\end{aligned} \tag{6}$$

where $\Lambda_1(i)$ and $\Lambda_B(i)$ will be defined later on, cf. see (11) and (12), (15) and (16), and (34) and (35).

IV. Uplink-Downlink Rate Region Maximization for Continuous-Rate Transmission

In this section, we assume that U1 and BS can adapt their transmission data rates in each time slot and transmit with the maximum possible data rates which do not cause outages on the underlying channels. Thereby, in this section, we assume that U1 and BS transmit with rates $R_1(i)=q_1(i)C_1(i)$ and $R_B(i)=q_B(i)C_B(i)$ in time slot i, respectively, where $C_1(i)$ and $C_B(i)$ are given in (1) and (2), respectively, and $q_1(i)$ and $q_B(i)$ are defined in (3) and (4), respectively.

In the following, we first define the uplink-downlink rate region and then propose two different schemes which maximize the rate region for the cases when U1 and BS both perform adaptive-power allocation in each time slot, and when U1 and BS both transmit with fixed powers in each time slot, respectively.

A. Rate Region Derivation

In time slot i, U1 transmits to the BS a codeword with rate $R_1(i)=C_1(i)$ if $q_1(i)=1$ and is silent otherwise. Similarly, the BS transmits to U2 a codeword with rate $R_B(i)=C_B(i)$ if $q_B(i)=1$ and is silent otherwise. Hence, the achieved rates during $N\to\infty$ time slots on the U1-BS and the BS-U2 channels, denoted by $\bar{R}_1$ and $\bar{R}_B$, respectively, are given by

$$\bar{R}_1=\lim_{N\to\infty}\frac{1}{N}\sum_{i=1}^{N}q_1(i)\log_2\left(1+P_1(i)\gamma_1(i)\right), \tag{7}$$

$$\bar{R}_B=\lim_{N\to\infty}\frac{1}{N}\sum_{i=1}^{N}q_B(i)\log_2\left(1+P_B(i)\gamma_B(i)\right). \tag{8}$$

The rate-pair $(\bar{R}_1, \bar{R}_B)$, given by (7) and (8), defines the boundary line of the uplink-downlink rate region. Our task in this section is to maximize the rate-pair $(\bar{R}_1, \bar{R}_B)$ and thereby obtain the maximum uplink-downlink rate region.

B. Adaptive-Power Allocation

In this subsection, we assume that U1 and BS can adapt their transmit powers, $P_1(i)$ and $P_B(i)$, in each time slot in order to maximize the boundary line of the uplink-downlink rate region $(\bar{R}_1, \bar{R}_B)$, such that the following long-term power constraints are satisfied

$$\lim_{N\to\infty} \frac{1}{N} \sum_{i=1}^{N} q_k(i) P_k(i) \leq \bar{P}_k, k \in \{1, B\}. \tag{9}$$

For this case, the maximum boundary line of the uplink-downlink rate region, $(\bar{R}_1, \bar{R}_B)$, defined by (7) and (8), can be obtained from the following optimization problem

$$\begin{aligned} &\underset{q_1(i), q_B(i), P_1(i), P_B(i)}{\text{Maximize:}} \ \mu \bar{R}_1 + (1-\mu)\bar{R}_B \\ &\text{Subject to :} \\ &\quad \text{C1} : q_k(i) \in \{0, 1\}, k \in \{1, B\} \\ &\quad \text{C2} : q_1(i) + q_B(i) \in \{0, 1\} \\ &\quad \text{C3} : \frac{1}{N} \sum_{i=1}^{N} q_k(i) P_k(i) \leq \bar{P}_k, k \in \{1, B\} \\ &\quad \text{C4} : P_k(i) \geq 0, k \in \{1, B\}, \end{aligned} \tag{10}$$

where C1 constrains the values that $q_1(i)$ and $q_B(i)$ can assume, C2 ensures that no more than one network state is active in each time slot, C3 ensures the long-term power constraints at U1 and BS are satisfied, and C4 ensures that the transmit powers $P_1(i)$ and $P_B(i)$ are non-negative. In (10), μ is a constant which satisfies $0 \leq \mu \leq 1$. A specific value of μ provides one point on the boundary line of the uplink-downlink rate region $(\bar{R}_1, \bar{R}_B)$. By varying μ from zero to one, the entire boundary line of the uplink-downlink rate region $(\bar{R}_1, \bar{R}_B)$ can be obtained. The solution of problem (10) is given in the following theorem.

Theorem 1: The optimal state-selection variables $q_1(i)$ and $q_B(i)$ maximizing the uplink-downlink rate region of the considered network with continuous-rate and adaptive-power transmission, which are found as the solution of (10), are given in (6), where $\Lambda_1(i)$ and $\Lambda_B(i)$ are

defined as

$$\Lambda_1(i) = \mu \log_2 (1 + P_1(i)\gamma_1(i)) - \zeta_1 P_1(i), \tag{11}$$

$$\Lambda_B(i) = (1-\mu) \log_2 (1 + P_B(i)\gamma_B(i)) - \zeta_B P_B(i), \tag{12}$$

where ζ_1 and ζ_B are constants found such that the constraint in C3 holds with equality for $k \in \{1, B\}$, respectively. On the other hand, the optimal transmit powers $P_1(i)$ and $P_B(i)$, found also as the solution of (10), are given by

$$P_k(i) = \begin{cases} \frac{\rho}{\lambda_k} - \frac{1}{\gamma_k(i)} & \text{if } \gamma_k(i) > \lambda_k/\rho, k \in \{1, B\} \\ 0 & \text{otherwise,} \end{cases} \tag{13}$$

where $\lambda_k \triangleq \frac{\zeta_k \ln(2)}{1-\mu}$, for $k \in \{1, B\}$ and $\rho \triangleq \frac{\mu}{1-\mu}$.

Proof: Please refer to Appendix A for the proof. ■

C. Fixed-Power Allocation

In this subsection, we assume that U1 and BS cannot perform adaptive-power allocation in each time slot. As a result, the transmit powers $P_1(i)$ and $P_B(i)$ are fixed during all time slots, i.e., $P_1(i) = P_1$ and $P_B(i) = P_B$, $\forall i$. However, the values of P_1 and P_B can still be optimized, such that the following long-term power constraints are satisfied

$$\lim_{N\to\infty} \frac{1}{N} \sum_{i=1}^{N} q_k(i) P_k \leq \bar{P}_k, k \in \{1, B\}. \tag{14}$$

For this case, the uplink-downlink rate region maximization problem for fixed-power allocation can be obtained by setting $P_1(i) = P_1$ and $P_B(i) = P_B$, $\forall i$, in (10). The solution of problem (10) with $P_1(i) = P_1$ and $P_B(i) = P_B$, $\forall i$, is given in the following theorem.

Theorem 2: The optimal state-selection variables $q_1(i)$ and $q_B(i)$ maximizing the uplink-downlink rate region of the considered network with continuous-rate and fixed-power transmission, found as the solution of (10) with $P_1(i) = P_1$ and $P_B(i) = P_B$, $\forall i$, are given in (6), where $\Lambda_1(i)$ and $\Lambda_B(i)$ are defined as

$$\Lambda_1(i) = \mu \log_2 (1 + P_1\gamma_1(i)) - \zeta_1 P_1, \tag{15}$$

$$\Lambda_B(i) = (1-\mu) \log_2 (1 + P_B\gamma_B(i)) - \zeta_B P_B, \tag{16}$$

where ζ_1 and ζ_B are constants found such that the constraint C3 in (10) with $P_1(i) = P_1$ and $P_B(i) = P_B$, $\forall i$, holds with equality for $k \in \{1, B\}$, respectively. Whereas, the optimal constant powers P_1 and P_B are found from the following equations

$$\lim_{N\to\infty} \frac{1}{N} \sum_{i=1}^{N} \left[\frac{\mu q_1(i)\gamma_1(i)}{\ln(2)(1+P_1\gamma_1(i))} - \zeta_1 q_1(i) \right] = 0, \tag{17}$$

and

$$\lim_{N\to\infty} \frac{1}{N} \sum_{i=1}^{N} \left[\frac{(1-\mu) q_B(i)\gamma_B(i)}{\ln(2)(1+P_B\gamma_B(i))} - \zeta_B q_B(i) \right] = 0, \tag{18}$$

respectively.

Proof: Please refer to Appendix B for the proof. ■

D. Practical Estimation of the Necessary Parameters

In order for the uplink-downlink scheduling schemes proposed in Theorems 1 and 2 to be employed in practice, certain amount of CSI is needed at U1, BS, and U2. In particular, at the start of time slot i, U1 and U2 need CSI of the U1-BS and the BS-U2 channels, respectively, whereas, the BS needs CSI of both U1-BS and BS-U2 channels[2]. Using the acquired CSI, U1 can compute $\Lambda_1(i)$ and $P_1(i)$, U2 can compute $\Lambda_B(i)$ and $P_B(i)$, whereas the BS can compute $\Lambda_1(i)$, $\Lambda_B(i)$, $P_1(i)$, and $P_B(i)$, using the expressions provided in Theorems 1 and 2. Consequently, the BS can compute the optimal state-selection variables $q_1(i)$ and $q_B(i)$ using (6), and then feedback the optimal state, $q_1(i) = 1$ or $q_B(i) = 1$, to U1 and U2 using one[3] bit of feedback information.

The computation of $\Lambda_1(i)$, $\Lambda_B(i)$, $P_1(i)$, and $P_B(i)$ also depends on acquiring the value of ζ_1 at U1 and BS, and acquiring the value of ζ_B at U2 and the BS. We note that the constants ζ_1 and ζ_B can be estimated in real-time using only instantaneous CSI of the local channel and employing the gradient descent method [25]. In particular, for the adaptive-power allocation scheme, the constants ζ_1 and ζ_B can be estimated as $\zeta_1^e(i)$ and $\zeta_B^e(i)$, respectively, using

$$\zeta_k^e(i+1) = \zeta_k^e(i) + \delta_k^{\zeta}(i) \left[\bar{P}_k^e(i) - \bar{P}_k \right], \, k \in \{1, B\}, \tag{19}$$

[2]The required CSI can be acquired by three transmissions of pilot symbols; one from each of the three nodes.

[3]If the state $q_1(i) = q_B(i) = 0$ occurs, then U1 can detect that $q_1(i) = 0$ has occurred by checking whether $\Lambda_1(i) < 0$ holds. Consequently, when $\Lambda_1(i) < 0$ holds, U1 should remain silent. Similarly, U2 can compute that $q_B(i) = 0$ has occurred by checking whether $\Lambda_B(i) < 0$ holds. Consequently, when $\Lambda_B(i) < 0$ holds, U2 should not receive. Hence, for the state $q_1(i) = q_B(i) = 0$, feedback from the BS to U1 and U2 is not required.

where $\delta_k(i)$ for $k \in \{1, B\}$ is an adaptive step size which controls the speed of convergence of $\zeta_k^e(i)$ to ζ_k, for $k \in \{1, B\}$, which can be some properly chosen monotonically decaying function of i with $\delta_k(1) < 1$. Moreover, in (19), $\bar{P}_1^e(i)$ and $\bar{P}_2^e(i)$ are real-time estimates of the average powers consumed at U1 and BS up to time slot i, respectively, obtained as

$$\bar{P}_k^e(i) = \frac{i-1}{i}\bar{P}_k^e(i-1) + \frac{1}{i}q_k(i)P_k(i),\ k \in \{1, B\}, \tag{20}$$

where $P_k(i)$, for $k \in \{1, B\}$, are given in Theorem 1.

On the other hand, for the proposed fixed-power allocation scheme, the estimation of the constants ζ_1 and ζ_B is identical to the adaptive-power allocation scheme, except that $P_1(i)$ and $P_B(i)$ in (20), are estimated as $P_1^e(i)$ and $P_B^e(i)$, respectively, as follows

$$P_k^e(i+1) = P_k^e(i) + \delta_k^P(i)\mathrm{E}_k(i),\ k \in \{1, B\}, \tag{21}$$

where $\mathrm{E}_1(i)$ and $\mathrm{E}_B(i)$, are given by

$$\mathrm{E}_1(i) = \frac{i-1}{i}\mathrm{E}_1(i-1) + \frac{1}{i}\left[\frac{\mu q_1(i)\gamma_1(i)}{\ln(2)(1+P_1^e(i)\gamma_1(i))} - \zeta_1^e(i)q_1(i)\right], \tag{22}$$

and

$$\mathrm{E}_B(i) = \frac{i-1}{i}\mathrm{E}_B(i-1) + \frac{1}{i}\left[\frac{(1-\mu)q_B(i)\gamma_B(i)}{\ln(2)(1+P_B^e(i)\gamma_B(i))} - \zeta_B^e(i)q_B(i)\right], \tag{23}$$

respectively, with $\mathrm{E}_k(0)$ and $P_k^e(0)$ for $k \in \{1, B\}$ initialized to zero. Hence, using this approach, the powers $P_1(i)$ and $P_B(i)$ vary at first for small i, but then converge to a fixed value as i becomes larger.

V. Uplink-Downlink Throughput Region Maximization for Discrete-Rate Transmission

In this section, we assume that U1 and BS do not have full CSI of their corresponding transmission links and/or have some others constraints which limit their ability to adapt the transmit rates arbitrarily in each time slot. Consequently, U1 and BS transmit their codewords with rates which are selected from discrete finite sets of date rates, denoted by $\mathcal{R}_1 = \{R_1^1, R_1^2, ..., R_1^M\}$ and $\mathcal{R}_B = \{R_B^1, R_B^2, ..., R_B^L\}$, respectively, where M and L denote the total number of non-zero data rates available for transmission at U1 and BS, respectively.

A. Uplink-Downlink Throughput Region for Discrete Transmission Rates

In order to model the uplink-receptions and downlink-transmissions for discrete data rates in time slot i, we introduce the binary variables $q_1^m(i)$, $m = 1, 2..., M$ and $q_B^l(i)$, for $l = 1, ..., L$, defined as

$$q_1^m(i) = \begin{cases} 1 & \text{if U1 transmits with rate } R_1^m \text{ to BS and BS is silent in time slot } i \\ 0 & \text{otherwise,} \end{cases} \tag{24}$$

$$q_B^l(i) = \begin{cases} 1 & \text{if BS transmits with rate } R_B^l \text{ to U2 and U1 is silent in time slot } i \\ 0 & \text{otherwise.} \end{cases} \tag{25}$$

Since the considered network can be in one and only one state in time slot i, the following has to hold

$$\sum_{m=1}^{M} q_1^m(i) + \sum_{l=1}^{L} q_B^l(i) \in \{0, 1\}, \tag{26}$$

where if $\sum_{m=1}^{M} q_1^j(i) + \sum_{l=1}^{L} q_B^l(i) = 0$ holds, then U1 and BS are both silent in time slot i.

Since the available transmission rates at U_1 and BS are discrete, outages can occur. An outage occurs if the data rate of the transmitted codeword is larger than the capacity of the underlaying channel. To model the outages on the U1-BS and the BS-U2 links, we introduce the following auxiliary binary variables, $O_1^m(i)$, for $m = 1, ..., M$, and $O_B^l(i)$, for $l = 1, ..., L$, respectively, defined as

$$O_1^m(i) = \begin{cases} 1 & \text{if } \log_2(1 + P_1\gamma_1(i)) \geq R_1^m \\ 0 & \text{if } \log_2(1 + P_1\gamma_1(i)) < R_1^m, \end{cases} \tag{27}$$

$$O_B^j(i) = \begin{cases} 1 & \text{if } \log_2(1 + P_B\gamma_B(i)) \geq R_B^l \\ 0 & \text{if } \log_2(1 + P_B\gamma_B(i)) < R_B^l. \end{cases} \tag{28}$$

Using $O_1^m(i)$, $\forall m$, we can obtain that in time slot i a codeword transmitted by U1 with rate R_1^m can be decoded correctly at the BS if and only if (iff) $q_1^m(i)O_1^m(i) > 0$ holds. Similarly, using $O_B^l(i)$, we can obtain that in time slot i a codeword transmitted by the BS with rate R_B^l can be decoded correctly at U2 iff $q_B^l(i)O_B^l(i) > 0$ holds. Thereby, the achieved throughputs during $N \to \infty$ time slots on the U1-BS and BS-U2 channels, denoted by $\bar{R}_1$ and $\bar{R}_B$, respectively,

are given by

$$\bar{R}_1 = \lim_{N\to\infty} \frac{1}{N} \sum_{i=1}^{N} \sum_{m=1}^{M} R_1^m q_1^m(i) O_1^m(i), \tag{29}$$

$$\bar{R}_B = \lim_{N\to\infty} \frac{1}{N} \sum_{i=1}^{N} \sum_{l=1}^{L} R_B^l q_B^l(i) O_B^l(i). \tag{30}$$

The throughput pair $(\bar{R}_1, \bar{R}_B)$, given by (29) and (30), represent the boundary line of the throughput region. Our task now is to find the maximum boundary line of the uplink-downlink throughput region, $(\bar{R}_1, \bar{R}_B)$, by selecting the optimal values of $q_1^m(i)$, $q_B^l(i)$, $\forall m, l, i$, and selecting the optimal fixed powers at U1 and BS, P_1 and P_B, respectively, such that the following long-term power constraints are satisfied

$$\lim_{N\to\infty} \frac{1}{N} \sum_{i=1}^{N} \sum_{m=1}^{M} q_1^m(i) P_1 \leq \bar{P}_1, \tag{31}$$

$$\lim_{N\to\infty} \frac{1}{N} \sum_{i=1}^{N} \sum_{l=1}^{L} q_B^l(i) P_B \leq \bar{P}_B. \tag{32}$$

The maximum boundary line of the uplink-downlink throughput region, $(\bar{R}_1, \bar{R}_B)$, can be found from the following maximization problem

$$\begin{aligned}
&\underset{q_1^m(i), q_B^l(i), P_1, P_B, \forall l,m,i.}{\text{Maximize:}} \quad \mu\bar{R}_1 + (1-\mu)\bar{R}_B \\
&\text{Subject to :} \\
&\quad \text{C1}: \ q_1^m(i) \in \{0,1\}, \forall m \\
&\quad \text{C2}: \ q_B^l(i) \in \{0,1\}, \forall l \\
&\quad \text{C3}: \ \sum_{m=1}^{M} q_1^m(i) + \sum_{l=1}^{L} q_B^l(i) \in \{0,1\} \\
&\quad \text{C4}: \ \lim_{N\to\infty} \frac{1}{N} \sum_{i=1}^{N} \sum_{m=1}^{M} q_1^m(i) P_1 \leq \bar{P}_1, \\
&\quad \text{C5}: \ \lim_{N\to\infty} \frac{1}{N} \sum_{i=1}^{N} \sum_{l=1}^{L} q_B^l(i) P_B \leq \bar{P}_B \\
&\quad \text{C6}: P_k \geq 0, k \in \{1, B\}.
\end{aligned} \tag{33}$$

The solution of this problem is given in the following theorem.

Theorem 3: Define $q_1(i) = q_1^{m^*}(i)$ and $q_B(i) = q_B^{l^*}(i)$, respectively, where $m^* = \arg\max_m\{R_1^m O_1^m(i)\}$ and $l^* = \arg\max_l\{R_B^l O_B^l(i)\}$. Then, the optimal state and rate selection variables, $q_1(i)$ and $q_B(i)$, maximizing the uplink-downlink throughput region of the considered network for the case when U1 and BS transmit from finite sets of discrete transmission rates are given in (6), where $\Lambda_1(i)$ and $\Lambda_B(i)$ are defined as

$$\Lambda_1(i) = \mu_1 \max_m\{R_1^m O_1^m(i)\} - \zeta_1 P_1, \tag{34}$$

$$\Lambda_B(i) = (1-\mu) \max_l\{R_B^l O_B^l(i)\} - \zeta_B P_B, \tag{35}$$

where the constants ζ_1 and ζ_B are found such that constraints C4 and C5 in (33) hold with equality, respectively. On the other hand, the optimal fixed-powers, P_1 and P_B, are found from the following equations

$$\lim_{N\to\infty}\frac{1}{N}\sum_{i=1}^{N}\left[\frac{\mu q_1(i)\gamma_1(i)\Big(\sum_{m=1}^{M} R_1^m\Delta_1^m(i) - \sum_{m=1}^{M-1} R_1^m\Delta_1^{m+1}(i)\Big)}{\ln(2)(1+P_1\gamma_1(i))} - \zeta_1 q_1(i)\right] = 0, \tag{36}$$

and

$$\lim_{N\to\infty}\frac{1}{N}\sum_{i=1}^{N}\left[\frac{(1-\mu) q_B(i)\gamma_B(i)\Big(\sum_{l=1}^{L} R_B^l\Delta_B^l(i) - \sum_{l=1}^{L-1} R_B^l\Delta_B^{l+1}(i)\Big)}{\ln(2)(1+P_B\gamma_B(i))} - \zeta_B q_B(i)\right] = 0, \tag{37}$$

respectively. In (36) and (37), $\Delta_k^j(i)$ is a function that assumes the value one if $\log_2(1+P_k\gamma_k(i-1)) \le R_k^j \le \log_2(1+P_k\gamma_k(i))$ holds for $k \in \{1, B\}$ and $j \in \{l, m\}$, and assumes the value zero otherwise.

Proof: Please refer to Appendix C for the proof. ■

B. Outage Probability

In the literature, the outage probability is usually derived assuming only a single available transmission rate at the transmitter, see [26]. Following this convention, in the following, we derive the outage probabilities of the U1-BS and BS-U2 links achieved with the proposed scheme in Theorem 3 for $M = L = 1$ and $R_1^1 = R_B^1 = R_0$.

In time slot i, an outage occurs on the U1-BS link if U1 is selected to transmit and the U1-BS link is too weak to support the rate R_0, i.e., $q_1^1(i) = 1$ and $O_1^1(i) = 0$, or if both U1 and BS are not selected for transmission in time slot i, i.e., if $q_1^1(i) = q_B^1(i) = 0$, since in that case the time

slot i is wasted. Similarly, in time slot i, an outage occurs on the BS-U2 link if BS is selected to transmit and the BS-U2 link is too weak to support the rate R_0, i.e., $q_B^1(i)=1$ and $O_B^1(i)=0$, or if both U1 and BS are not selected for transmission in time slot i, i.e., if $q_1^1(i)=q_B^1(i)=0$, since in that case again the time slot i is wasted. Denoting the outage probability of the U1-BS link by $P_{\text{out,1}}$, we have

$$\begin{aligned} P_{\text{out,1}} &= \Pr\{[q_1^1(i)=1 \text{ AND } O_1^1(i)=0] \text{ OR } q_1^1(i)=q_B^1(i)=0\} \\ &\overset{(a)}{=} \Pr\{q_1^1(i)=1 \text{ AND } O_1^1(i)=0\} + \Pr\{q_1^1(i)=q_B^1(i)=0\}, \end{aligned} \tag{38}$$

where (a) follows since the events $q_1^1(i)=1$ and $q_1^1(i)=0$ are mutually exclusive. Similarly, the outage probability of the BS-U2 link, denoted by $P_{\text{out,B}}$, can be obtained as

$$\begin{aligned} P_{\text{out,B}} &= \Pr\{[q_B^1(i)=1 \text{ AND } O_B^1(i)=0] \text{ OR } q_1^1(i)=q_B^1(i)=0\} \\ &= \Pr\{q_B^1(i)=1 \text{ AND } O_B^1(i)=0\} + \Pr\{q_1^1(i)=q_B^1(i)=0\}. \end{aligned} \tag{39}$$

The outage probabilities $P_{\text{out,1}}$ and $P_{\text{out,B}}$ can be obtained by a Monte Carlo simulation. Thereby, it can be seen that the slope of the outage probabilities is -2 for Rayleigh fading, which means that the proposed scheme achieves a diversity gain of two on both the U1-BS and BS-U2 links. Note that the FDD-BS achieves a diversity gain of one for Rayleigh fading on both the uplink and downlink links. Hence, the proposed scheme doubles the diversity gain on both the uplink and downlink channels compared to a FDD-BS.

We can prove mathematically a diversity gain of two for Rayleigh fading only for the case when $\mu=1/2$, the fadings on the U1-BS and BS-U2 links are independent and identically distributed (i.i.d), and the average transmit powers at U1 and BS are identical, i.e., $\bar{P}_1=\bar{P}_B$ holds. In that case, $\zeta_1=\zeta_B=\zeta$ and $P_1=P_B=P$ in (34) and (35), and thereby $\Lambda_1(i)$ and $\Lambda_B(i)$ in (34) and (35) simplify to

$$\Lambda_k(i)=\frac{1}{2}R_0O_k(i)-\zeta P,\ k\in\{1,B\}. \tag{40}$$

Now, inserting $\Lambda_1(i)$ and $\Lambda_B(i)$ from (40) into (6), we obtain that $q_1^1(i)=1$ if $O_1^1(i)\geq O_B^1(i)$ and $O_1^1(i)>0$, which means that $q_1^1(i)=1$ occurs if $O_1^1(i)=1$. Hence, the event $q_1^1(i)=1$ and $O_1^1(i)=0$ is an impossible event, thereby leading to $\Pr\{q_B^1(i)=1 \text{ AND } O_B^1(i)=0\}=0$ in (38). Furthermore, we obtain that $q_1^1(i)=q_B^1(i)=0$ occurs iff $O_1^1(i)=O_B^1(i)=0$ holds,

thereby leading to $\Pr\{q_1^1(i)=q_B^1(i)=0\}=\Pr\{O_1^1(i)=0 \text{ AND } O_B^1(i)=0\}$ in (38). Inserting this into (38), we obtain

$$\begin{aligned} P_{\text{out},1} &= \Pr\{O_1^1(i)=0 \text{ AND } O_B^1(i)=0\} \\ &= \Pr\{\log_2(1+P\gamma_1(i))<R_0 \text{ AND } \log_2(1+P\gamma_B(i))<R_0\} \\ &= \Pr\{\gamma_1(i)<\gamma_{\text{th}} \text{ AND } \gamma_B(i)<\gamma_{\text{th}}\}, \end{aligned} \tag{41}$$

where $\gamma_{\text{th}}=\frac{2^{R_0}-1}{P}$. Now, from (41) it is clear that for Rayleigh fading, $P_{\text{out},1}$ has a diversity gain of two. Similar derivation can be performed for $P_{\text{out,B}}$.

C. Practical Estimation of the Necessary Parameters

In order for the uplink-downlink scheduling scheme proposed in Theorem 3 to be employed in practice, certain amount of CSI and feedback is again needed at U1, BS, and U2. In particular, at the start of time slot i, BS and U2 need CSI of the U1-BS and the BS-U2 channels[4], respectively. Using the acquired CSI, the BS can compute $\Lambda_1(i)$ using (34). On the other hand, U2 can compute $\max\limits_l\{R_B^l O_B^l(i)\}$ and feedback this information using $\log_2 L$ bits of information to the BS. Consequently, using the feedback information, the BS can compute $\Lambda_B(i)$ using (35). Thereby, using $\Lambda_1(i)$ and $\Lambda_B(i)$, the BS can compute the values of $q_1^m(i)$ and $q_B^l(i)$ using (24) and (25), respectively, and can then feedback this information using $\log_2(L+M)$ bits of information to U1 and U2. Using the feedback information, U1 and U2 can become aware if they need to transmit and receive, respectively, with a certain rate in time slot i.

The computation of $\Lambda_1(i)$, $\Lambda_B(i)$, P_1, and P_B depends on obtaining the value of ζ_1 at the BS, and obtaining the value of ζ_B at U2. The constants ζ_1 and ζ_B can be estimated in real-time using only instantaneous CSI of the local channel and employing the gradient descent method [25]. In particular, for the uplink-downlink scheduling scheme proposed in Theorem 3, the constants ζ_1 and ζ_B can be estimated as $\zeta_1^e(i)$ and $\zeta_B^e(i)$, respectively, using (19), where $\bar{P}_1^e(i)$ and $\bar{P}_B^e(i)$, are given by (20). In (20), $P_1^e(i)$ and $P_B^e(i)$, are obtained using (21), where $\text{E}_1(i)$ and $\text{E}_B(i)$ are

[4]The required CSI can be acquired by two transmissions of pilot symbols; one from U1 and one from BS.

given by

$$\mathrm{E}_1(i) = \frac{i-1}{i}\mathrm{E}_1(i-1) + \frac{1}{i}\left[\frac{(\mu q_1(i)\gamma_1(i)\Big(\sum_{m=1}^{M} R_1^m \Delta_1^m(i) - \sum_{m=1}^{M-1} R_1^m \Delta_1^{m+1}(i)\Big)}{\ln(2)(1+P_1^e(i)\gamma_1(i))} - \zeta_1^e(i) q_1(i)\right], \quad (42)$$

$$\mathrm{E}_B(i) = \frac{i-1}{i}\mathrm{E}_B(i-1) + \frac{1}{i}\left[\frac{(1-\mu) q_B(i)\gamma_B(i)\Big(\sum_{l=1}^{L} R_B^l \Delta_B^l(i) - \sum_{l=1}^{L-1} R_B^l \Delta_B^{l+1}(i)\Big)}{\ln(2)(1+P_B^e(i)\gamma_B(i))} - \zeta_B^e(i) q_B(i)\right], \quad (43)$$

respectively, where the definition of all other necessary parameters are given in Section V-A.

VI. Fairness

Fairness is always a concern when two users compete for a limited resource. In the proposed schemes, the fairness between the uplink and downlink rates/throughputs can be controlled via the constant $0 \leq \mu \leq 1$. If $\mu = 1$ is set, then the BS always receives from U1, thereby maximizing the uplink rate/throughput from U1 to BS and diminishing the downlink rate/throughput from BS to U2 to zero. Contrary, if $\mu = 0$ is set, then the BS always transmits to U2, thereby maximizing the downlink rate/throughput from BS to U2 and diminishing the uplink rate/throughput from U1 to BS to zero. By varying μ from one to zero, we steer the priority from U1 to U2, and thereby obtain any desired fairness. However, with the proposed schemes in Theorems 1-3, it is not a priori clear which value should μ assume in order to obtain a desired level of fairness. In the following, we propose two different types of fairness between U1 and U2, and then propose corresponding practical schemes for achieving the desired fairness in real-time by adjusting the value of μ.

A. Prioritized Fairness

In this case, we want the uplink rate/throughput between U1 and the BS, $\bar{R}_1$, given by (7) for continuous-rate transmission and given by (29) for discrete-rate transmission, to be equal to some desired rate, denoted by $\bar{R}_{1,\mathrm{des}}$, i.e., $\bar{R}_1 = \bar{R}_{1,\mathrm{des}}$ to hold. To obtain $\bar{R}_1 = \bar{R}_{1,\mathrm{des}}$, we

propose the value of μ in time slot i to be set to $\mu = \mu^e(i)$, where $\mu^e(i)$ is obtained as

$$\mu^e(i+1) = \mu^e(i) + \delta(i)\left[\bar{R}_1^e(i) - \bar{R}_{1,\mathrm{des}}\right]. \tag{44}$$

In (44), $\bar{R}_1^e(i)$ is given by

$$\bar{R}_1^e(i) = \frac{i-1}{i}\bar{R}_1^e(i-1) + \frac{1}{i}R_1(i), \tag{45}$$

where $R_1(i) = q_1(i)\log_2\left(1 + P_1(i)\gamma_1(i)\right)$ for continuous-rate transmission and $R_1(i) = \sum_{m=1}^{M} R_1^m q_1^m(i) O_1^m(i)$ for discrete-rate transmission.

B. Proportional Fairness

In this case, we want $\bar{R}_1 = \alpha\bar{R}_2$ to hold, where α is a desired proportional level between the uplink and downlink rates/throughputs. To obtain $\bar{R}_1 = \alpha\bar{R}_2$, we propose the value of μ in time slot i to be set to $\mu = \mu^e(i)$, where $\mu^e(i)$ is obtained as

$$\mu^e(i+1) = \mu^e(i) + \delta(i)\left[\bar{R}_1^e(i) - \alpha\bar{R}_B^e(i)\right]. \tag{46}$$

In (46), $\bar{R}_1^e(i)$ and $\bar{R}_B^e(i)$ are obtained as

$$\bar{R}_k^e(i) = \frac{i-1}{i}\bar{R}_k^e(i-1) + \frac{1}{i}R_k(i), k \in \{1, B\}, \tag{47}$$

where $R_1(i)$ and $R_B(i)$ are given by

$$R_k(i) = q_k(i)\log_2\left(1 + P_k(i)\gamma_k(i)\right),\ k \in \{1, B\}, \tag{48}$$

for continuous-rate transmission, and

$$R_1(i) = \sum_{m=1}^{M} R_1^m q_1^m(i) O_1^m(i), \text{ and } R_B(i) = \sum_{l=1}^{L} R_B^l q_B^l(i) O_B^l(i), \tag{49}$$

for discrete-rate transmission.

VII. Simulation And Numerical Results

In this section, we evaluate the performance of the proposed schemes, and then compare it to the performance achieved with a FDD-BS. To this end, we first introduce the FDD-BS benchmark scheme and then present the numerical results.

A. Benchmark Scheme (FDD-BS)

The FDD-BS receives and transmits in different frequency bands, receptively. Assuming that the fraction of bandwidth allocated for uplink and downlink is μ and $1-\mu$, respectively, the boundary line of the achieved rate region during $N \to \infty$ time slots, $(\bar{R}_1, \bar{R}_B)$, is given by

$$\bar{R}_1 = \lim_{N\to\infty} \frac{\mu}{N} \sum_{i=1}^{N} \log_2 \left(1 + \frac{\bar{P}_1}{\mu}\gamma_1(i)\right), \tag{50}$$

$$\bar{R}_B = \lim_{N\to\infty} \frac{1-\mu}{N} \sum_{i=1}^{N} \log_2 \left(1 + \frac{\bar{P}_B}{1-\mu}\gamma_B(i)\right). \tag{51}$$

On the other hand, the boundary line of the throughput region during $N \to \infty$ time slots, assuming single transmission rates at U1 and BS, is given by

$$\bar{R}_1 = \lim_{N\to\infty} \frac{\mu}{N} \sum_{i=1}^{N} O_1^1(i) R_1^1, \tag{52}$$

$$\bar{R}_B = \lim_{N\to\infty} \frac{1-\mu}{N} \sum_{i=1}^{N} O_B^1(i) R_B^1, \tag{53}$$

where $O_1^1(i)$ and $O_B^1(i)$ are defined as

$$O_1^1(i) = \begin{cases} 1 & \text{if } \log_2\left(1 + \frac{\bar{P}_1}{\mu}\gamma_1(i)\right) \geq R_1^1 \\ 0 & \text{if } \log_2\left(1 + \frac{\bar{P}_1}{\mu}\gamma_1(i)\right) < R_1^1, \end{cases} \tag{54}$$

$$O_B^1(i) = \begin{cases} 1 & \text{if } \log_2\left(1 + \frac{\bar{P}_B}{1-\mu}\gamma_B(i)\right) \geq R_B^1 \\ 0 & \text{if } \log_2\left(1 + \frac{\bar{P}_B}{1-\mu}\gamma_B(i)\right) < R_B^1. \end{cases} \tag{55}$$

Remark 2: Note that the boundary line of the rate region defined by $(\bar{R}_1, \bar{R}_B)$ in (50) and (51), and the throughput region defined by $(\bar{R}_1, \bar{R}_B)$ in (52) and (53), are also the boundary lines of the corresponding rate and throughput regions achieved by a user with decoupled *out-of-band* uplink-transmissions to BS2 and downlink-receptions from BS1, cf. Fig. 2, where the fraction of bandwidth allocated for uplink and downlink is μ and $1-\mu$, respectively.

Remark 3: Note that the boundary line of the rate region defined by $(\bar{R}_1, \bar{R}_B)$ in (50) and (51), and the throughput region defined by $(\bar{R}_1, \bar{R}_B)$ in (52) and (53), are also the boundary lines of the corresponding rate and throughput regions achieved by a BS (or a user) which employs in-band but *non-adaptive* receptions and transmissions in fractions μ and $1-\mu$ of the

total number of time slots, receptively, e.g. uplinks in the first μN and downlinks in following $(1-\mu)N$ time slots.

B. Numerical Results

All of the presented results in this section have been performed by numerical evaluation of the derived results and are confirmed by Monte Carlo simulations. Moreover, Rayleigh fading is assumed.

1) Simulation Parameters: For the numerical example shown in Fig. 3, the mean of the channel gains of the U1-BS and BS-U2 links are calculated using the standard path-loss model as

$$E\{|h_L(i)|^2\} = \left(\frac{c}{4\pi f_c}\right)^2 d_L^{-\beta} \text{ , for } L \in \{1, B\}, \tag{56}$$

where c is the speed of light, f_c is the carrier frequency, d_L is the distance between the transmitter and the receiver of link L, and β is the path loss exponent. For this example, the carrier frequency is set to $f_c = 1.9$ GHz. Moreover, we assume $\beta = 3.6$ for the U1-BS and BS-U2 channels. Also, we assume that the transmit bandwidth is 200 kHz. Moreover, users have ominidirectional antenna with unity gain, and the BS has a directional antenna with gain of 16 dBi. The power at U1 is set to 24 dBm and the power at BS is set to 46 dBm. The distances between U1 and BS, as well as BS and U2, are assumed to be fixed and is set to 700m. The noise figure of BS and U2 are set to 2 dB and 7 dB, respectively. The above parameters reflect the parameters used in practice.

On the other hand, for the numerical examples shown in Fig. 4-7, users and the BS are asumied to have ominidirectional antennas with unity gain and same noise level. For these examples, the signal to noise ratio (SNR) is defined as the ratio of the average received power and the noise power.

Finally, for the numerical examples with discrete-rates schemes in Fig. 3-7, we assume $M = L$ and $R_1^k = R_B^k = kR$, for $k = 1, 2, ..., M$, where R is defined differently depending on the example.

2) Rate/Throughput Region: In Fig. 3, we illustrate the rate region achieved using the proposed schemes for continuous-rate transmission with adaptive- and fixed-power allocation, as well as the throughput region for discrete-rate transmission with $M = 1$. Furthermore, we show the

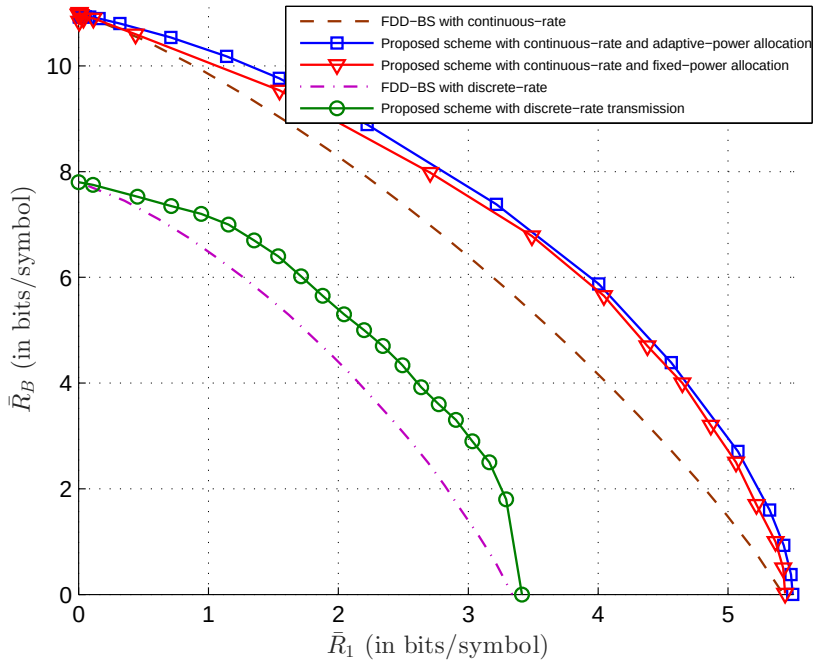

Fig. 3. Rate/throughput regions of the proposed schemes and the benchmark schemes.

rate/throughput regions achieved with the FDD benchmark scheme. For the proposed and the benchmark scheme with discrete-rate transmission, the value of R_k, for $k \in \{1, B\}$, is optimized numerically for a given μ, such that the throughput is maximized. As can be seen from Fig. 3, the proposed schemes achieve substantial gains compared to the FDD benchmark scheme. For example, the proposed continuous-rate transmission schemes with adaptive- and fixed-power allocation have an uplink rate gain of about 22%, 27% and 63%, compared to the benchmark scheme for a downlink rate of 6, 8, and 10 bits/symb, respectively. For the proposed scheme with discrete-rate transmission, we have an uplink throughput gain of about 20%, 29% and 67%, compared to the benchmark scheme for downlink throughput of 3, 5, and 7 bits/symb, respectively.

Fig. 3 clearly shows the superior performance of a BS employing adaptive scheduling of the in-band uplink-receptions and downlink-transmissions compared to the performance of a FDD-BS. Consequently, Fig. 3 also shows the superior performance of user employing adaptive scheduling of the *in-band* uplink-transmission and downlink-receptions to/from two BSs, cf. Fig. 2, compared to the performance of a user employing *out-of-band* uplink-receptions and downlink-transmissions from two BSs or a user with coupled uplink-downlink transmission to

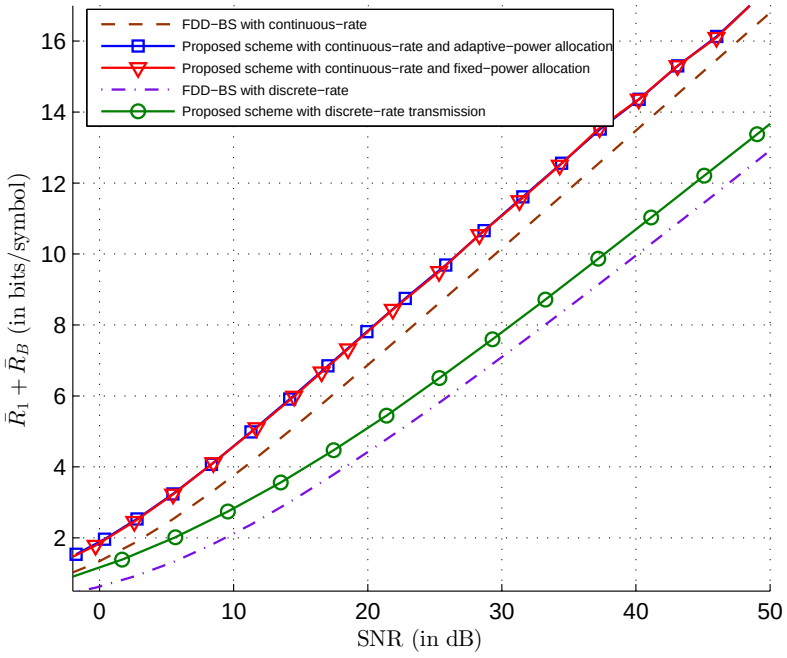

Fig. 4. Data rate/throughput vs. SNR of the proposed schemes and the benchmark schemes.

a single BS.

3) Sum-Rate Capacity: In Fig. 4, we show the sum of the uplink and downlink rates/throughputs achieved with the proposed schemes with continuous-rate with adaptive- and fixed-power allocation, with discrete-rate transmission for $M = 1$, and with the benchmark schemes as a function of the SNR. For the schemes with discrete-rate transmission the value of R_k, for $k \in \{1, B\}$, is optimized numerically, for a given SNR, such that the throughput is maximized. As can be seen, the performance of the proposed schemes have a considerable gains compared to the benchmark schemes. For example, the proposed continuous-rate transmission schemes with adaptive-power allocation and fixed-power allocation have a sum-rate gains of about 46%, 29% and 19%, compared to the benchmark scheme for SNR values of 0dB, 7dB, and 15dB, respectively. For the proposed scheme with discrete-rate transmission, we have a throughput gain of about 100%, 50% and 26%, compared to the FDD benchmark scheme for SNR values of 0dB, 7dB, and 15dB, respectively. Moreover, it can be seen that the proposed schemes provide around 3 dB SNR gain compared to the FDD benchmark scheme.

In Fig. 5, we show the sum of the uplink and downlink throughputs achieved with the proposed scheme for discrete-rate transmission as a function of the SNR for $M = 1, 4, 16, \infty$, where R

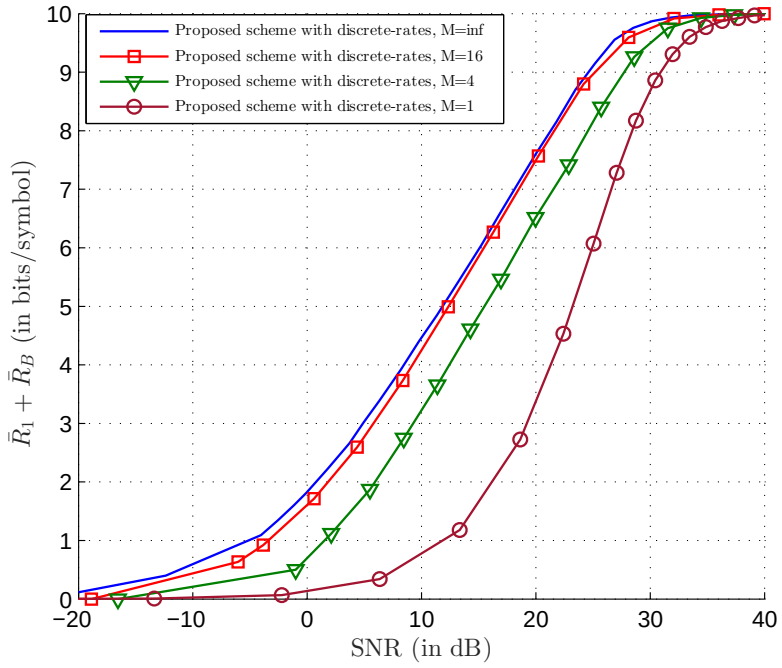

Fig. 5. Data rate/throughput vs. SNR of the proposed scheme with discrete-rates transmission.

is set to $R = 10/M$ bits/symb. It can be concluded from Fig. 5 that by increasing M from 1 to 4 we can gain more than 10 dBs in the SNR for around 5 bits/symb sum throughput. Also, by increasing M from 4 to 16 we can gain an additional 3 dBs in the SNR for around 5 bits/symb of the sum throughput. Finally, Fig. 5 shows that the proposed scheme with discrete-rates transmission for $M = 16$ performs very close to the one with $M = \infty$.

4) Outage Probability: In Fig. 6, we illustrate the outage probabilities of the proposed scheme with discrete-rate transmission and the FDD benchmark scheme as a function of the SNR for $M = 1$, where R is set to $R = 1$ bits/symb. Fig. 6 shows that the outage probability achieved with the proposed scheme decays with double the slope compared to the outage probability achieved with the FDD benchmark scheme, i.e, a diversity gain of two is achieved by the proposed scheme compared to a diversity gain of one with the FDD benchmark scheme, which was predicted theoretically in Section V-B. This leads to significant SNR gains. For example, SNR gains of 10dB and 15dB can be achieved for outage probabilities of 0.01 and 0.001, respectively.

5) Fairness: In Fig. 7, we demonstrate the uplink-downlink rates achieved using the proposed continuous-rate with adaptive-power allocation scheme with prioritized and proportional fairness as a function of the time slot i. For prioritized fairness, the desired uplink-rate is set to $\bar{R}_{1,\text{des}} = 5$

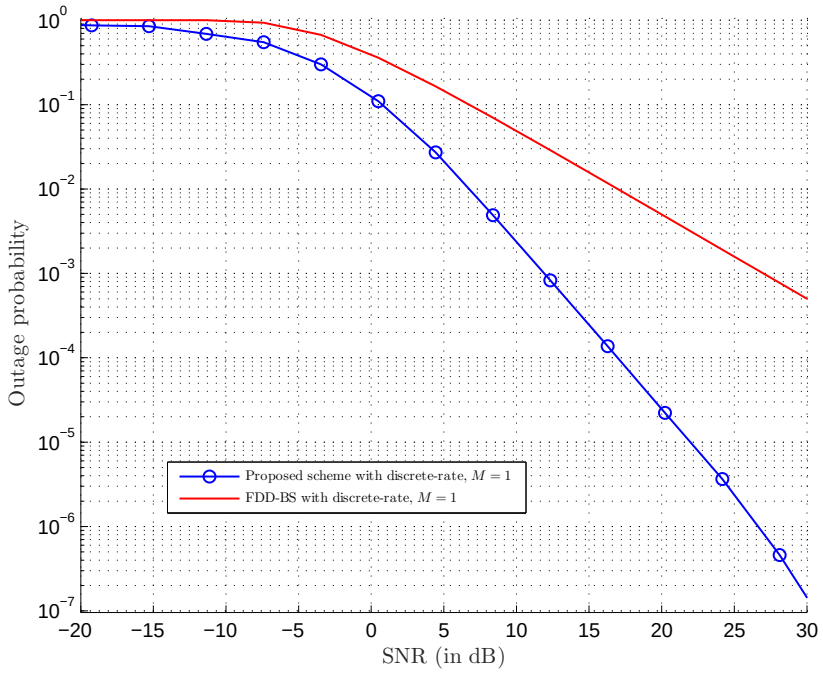

Fig. 6. Outage probability vs. SNR of the proposed scheme with discrete-rates transmission.

bits/symb, and for proportional fairness the value of the desired proportional level, α, is set to $\alpha = 5$. Moreover, the SNR is set to 15 dB. As can be seen from Fig. 7, the proposed schemes in Section VI-B, achieve the desired level of fairness.

VIII. Conclusion

In this paper, we proposed a novel reception/transmission scheme for half-duplex BSs. Using the proposed schemes, the BS can adaptively select to either receive from user 1 or to transmit to user 2 in a given time slot based on the qualities of the in-band uplink-reception and downlink-transmission channels, such that the uplink-downlink rate/throughput region is maximized. We have showed that the proposed BS with adaptive scheduling of the in-band uplink-receptions and downlink-transmissions provides significant performance gains compared to the conventional FDD base station. In particular, we have shown an increase in the uplink-downlink rate/throughput region and doubling of the diversity gain on both the uplink and downlink links. An implicit consequence of the results in this paper is that both the BSs and the users in a cellular network should employ adaptive scheduling of the *in-band* receptions and transmissions from different users and BSs, respectively, as proposed in this paper, in order to

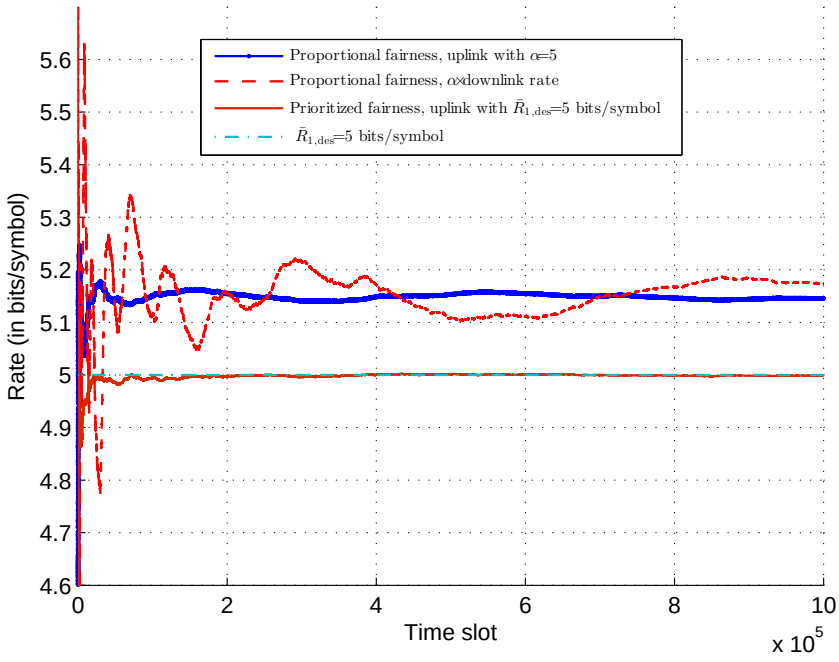

Fig. 7. Uplink-downlink rates vs. time slots of the proposed adaptive-power scheme with prioritized and proportional fairness.

harness the available diversity gains of the cellular network.

APPENDIX

A. *Proof of Theorem 1*

We relax the constraints C2 and C3, ignore C4, and then use the Lagrangian. Thereby, with some simplification we can obtain

$$\begin{aligned}\mathcal{L} \;&= \mu q_1(i)\log_2\left(1+P_1(i)\gamma_1(i)\right) + (1-\mu)q_B(i)\log_2\left(1+P_B(i)\gamma_B(i)\right)\\ &-\zeta_1 q_1(i)P_1(i) - \zeta_B q_B(i)P_B(i)\\ &-\lambda_1(i)q_1(i) - \lambda_2(i)\left(1-q_1(i)\right) - \lambda_3(i)q_B(i) - \lambda_4(i)\left(1-q_B(i)\right)\\ &-\lambda_5(i)\left(q_1(i)+q_B(i)\right) - \lambda_6(i)\left(1-q_1(i)-q_B(i)\right),\end{aligned} \tag{57}$$

where $\zeta_1 \geq 0$, $\zeta_B \geq 0$, and $\lambda_k \geq 0$, $\forall k$, are the Lagrangian multipliers. By differentiating $\mathcal{L}$ with respect to $P_1(i)$ and $P_B(i)$, and then setting the result to zero, we obtain

$$\frac{d\mathcal{L}}{dP_1(i)} = \frac{\mu q_1(i)\gamma_1(i)}{\ln(2)\left(1+P_1(i)\gamma_1(i)\right)} - \zeta_1 q_1(i) = 0, \tag{58}$$

$$\frac{d\mathcal{L}}{dP_B(i)} = \frac{(1-\mu) q_B(i)\gamma_B(i)}{\ln(2)\left(1+P_B(i)\gamma_B(i)\right)} - \zeta_B q_B(i) = 0. \tag{59}$$

Now, we calculate $P_1(i)$ and $P_B(i)$ from (58) and (59), receptively. For $q_1(i) = 1$, (58) becomes

$$\frac{d\mathcal{L}}{dP_1(i)} = \frac{\mu\gamma_1(i)}{\ln(2)\,(1 + P_1(i)\gamma_1(i))} - \zeta_1 = 0. \tag{60}$$

Solving (60), we can obtain $P_1(i)$ as in (13). For $q_B(i) = 1$, (59) becomes

$$\frac{d\mathcal{L}}{dP_B(i)} = \frac{(1-\mu)\gamma_B(i)}{\ln(2)\,(1 + P_B(i)\gamma_B(i))} - \zeta_B = 0. \tag{61}$$

Solving (61), we can obtain $P_B(i)$ as in (13). Finally, using (57) and defining $-\lambda_5(i) + \lambda_6(i) \triangleq -\beta(i)$, we can find the state-selection scheme as follows. The conditions which maximize (57), in the cases when $q_1(i) = 1$ and $q_B(i) = 0$, are

$$\mu \log_2 (1 + P_1(i)\gamma_1(i)) - \zeta_1 P_1(i) - \beta(i) > 0, \tag{62}$$

and

$$(1-\mu) \log_2 (1 + P_B(i)\gamma_B(i)) - \zeta_B P_B(i) - \beta(i) < 0. \tag{63}$$

Similarly, maximizing (57), for the cases when $q_1(i) = 0$ and $q_B(i) = 1$, the following conditions must hold

$$\mu \log_2 (1 + P_1(i)\gamma_1(i)) - \zeta_1 P_1(i) - \beta(i) < 0, \tag{64}$$

and

$$(1-\mu) \log_2 (1 + P_B(i)\gamma_B(i)) - \zeta_B P_B(i) - \beta(i) > 0. \tag{65}$$

In (62)-(65), we can substitute $\mu \log_2 (1 + P_1(i)\gamma_1(i)) - \zeta_1 P_1(i)$ with $\Lambda_1(i)$ and $(1-\mu)\log_2(1+ P_B(i)\gamma_B(i)) - \zeta_B P_B(i)$ with $\Lambda_B(i)$, and obtain the state-selection scheme. This completes the proof.

B. Proof of Theorem 2

We relax the constraints C2 and C3, and ignore C4. Then, we use the Lagrangian. Thereby, we obtain

$$\begin{aligned}\mathcal{L} &= \lim_{N\to\infty} \tfrac{1}{N} \textstyle\sum_{i=1}^{N} \mu q_1(i) \log_2\left(1 + P_1\gamma_1(i)\right) \\ &+ \lim_{N\to\infty} \tfrac{1}{N} \textstyle\sum_{i=1}^{N} (1-\mu) q_B(i) \log_2\left(1 + P_B\gamma_B(i)\right) \\ &- \tfrac{1}{N} \textstyle\sum_{i=1}^{N} \zeta_1 q_1(i) P_1 - \tfrac{1}{N} \textstyle\sum_{i=1}^{N} \zeta_B q_B(i) P_B \\ &- \lambda_1(i) q_1(i) - \lambda_2(i)(1 - q_1(i)) - \lambda_3(i) q_B(i) - \lambda_4(i)(1 - q_B(i)) \\ &- \lambda_5(i)\left(q_1(i) + q_B(i)\right) - \lambda_6(i)\left(1 - q_1(i) - q_B(i)\right), \end{aligned} \tag{66}$$

where $\zeta_1 \geq 0$, $\zeta_B \geq 0$, and $\lambda_k \geq 0$, $\forall k$, are the Lagrangian multipliers. By differentiating $\mathcal{L}$ with respect to P_1 and P_B, and setting the result to zero we obtain (17).

Furthermore, using (66) and defining $-\lambda_5(i) + \lambda_6(i) \triangleq -\beta(i)$, we can find the state-selection scheme as follows. The conditions which maximizes (66), for the cases when $q_1(i) = 1$ and $q_B(i) = 0$, are

$$\mu \log_2\left(1 + P_1\gamma_1(i)\right) - \zeta_1 P_1 - \beta(i) > 0, \tag{67}$$

and

$$(1-\mu) \log_2\left(1 + P_B\gamma_B(i)\right) - \zeta_B P_B - \beta(i) < 0. \tag{68}$$

For maximizing (66) in the cases when $q_1(i) = 0$ and $q_B(i) = 1$, the following conditions must hold

$$\mu \log_2\left(1 + P_1\gamma_1(i)\right) - \zeta_1 P_1 - \beta(i) < 0, \tag{69}$$

and

$$(1-\mu) \log_2\left(1 + P_B\gamma_B(i)\right) - \zeta_B P_B - \beta(i) > 0. \tag{70}$$

In (67)-(70), we can substitute $\mu \log_2\left(1 + P_1\gamma_1(i)\right) - \zeta_1 P_1$ with $\Lambda_1(i)$ and $(1-\mu) \log_2\left(1 + P_B\gamma_B(i)\right) - \zeta_B P_B$ with $\Lambda_B(i)$, and thereby obtain the state-selection scheme. This completes the proof.

C. Proof of Theorem 3

We relax the constraints C1 and C2, and ignore C4. Then we use the Lagrangian. Thereby, we obtain

$$\begin{aligned}\mathcal{L} &= \lim_{N\to\infty}\tfrac{1}{N}\textstyle\sum_{i=1}^{N}\sum_{m=1}^{M}\mu R_1^m q_1^m(i)O_1^m(i)\\ &+\lim_{N\to\infty}\tfrac{1}{N}\textstyle\sum_{i=1}^{N}\sum_{l=1}^{L}(1-\mu)R_B^l q_B^l(i)O_B^l\\ &-\lim_{N\to\infty}\tfrac{1}{N}\textstyle\sum_{i=1}^{N}\sum_{m=1}^{M}\zeta_1 q_1^m(i)P_1-\lim_{N\to\infty}\tfrac{1}{N}\textstyle\sum_{i=1}^{N}\sum_{l=1}^{L}\zeta_B q_B^l(i)P_B\\ &-\textstyle\sum_{m=1}^{M}\lambda_1^m(i)q_1^m(i)-\left(1-\sum_{m=1}^{M}\lambda_2^m(i)q_1^m(i)\right)\\ &-\textstyle\sum_{l=1}^{L}\lambda_3^l(i)q_B^l(i)-\left(1-\sum_{l=1}^{L}\lambda_4^l(i)q_B^l(i)\right)\\ &-\lambda_5(i)\left(\sum_{m=1}^{M}q_1^m(i)+\sum_{l=1}^{L}q_B^l(i)\right)-\lambda_6(i)\left(1-\sum_{m=1}^{M}q_1^m(i)-\sum_{l=1}^{L}q_B^l(i)\right),\end{aligned}\tag{71}$$

where $\zeta_1\geq 0$, $\zeta_B\geq 0$, and $\lambda_k(i)\geq 0$, $\forall k,i$, are the Lagrangian multipliers. we can rewrite (71) as

$$\begin{aligned}\mathcal{L} &= \lim_{N\to\infty}\tfrac{1}{N}\textstyle\sum_{i=1}^{N}\mu q_1(i)\max_m\{R_1^m O_1^m(i)\}\\ &+\lim_{N\to\infty}\tfrac{1}{N}\textstyle\sum_{i=1}^{N}(1-\mu)q_B(i)\max_l\{R_B^l O_B^l(i)\}\\ &-\lim_{N\to\infty}\tfrac{1}{N}\textstyle\sum_{i=1}^{N}\zeta_1 q_1(i)P_1-\lim_{N\to\infty}\tfrac{1}{N}\textstyle\sum_{i=1}^{N}\zeta_B q_B(i)P_B\\ &-\textstyle\sum_{m=1}^{M}\lambda_1^m(i)q_1^m(i)-\left(1-\sum_{m=1}^{M}\lambda_2^m(i)q_1^m(i)\right)\\ &-\textstyle\sum_{l=1}^{L}\lambda_3^l(i)q_B^l(i)-\left(1-\sum_{l=1}^{L}\lambda_4^l(i)q_B^l(i)\right)\\ &-\lambda_5(i)\left(q_1(i)+q_B(i)\right)-\lambda_6(i)\left(1-q_1(i)-q_B(i)\right).\end{aligned}\tag{72}$$

In order to determine P_1 and P_B, first we note that $\max_m\{R_1^m O_1^m(i)\}$ and $\max_l\{R_B^l O_B^l(i)\}$ can be rewritten in the following manners

$$\begin{aligned}\max_m\{R_1^m O_1^m(i)\} &= \sum_{m=1}^{M}R_1^m U[\log_2(1+P_1\gamma_1(i))-R_1^m]\\ &-\sum_{m=1}^{M-1}R_1^m U[\log_2(1+P_1\gamma_1(i))-R_1^{m+1}],\end{aligned}\tag{73}$$

$$\max_{l}\{R_B^l O_B^l(i)\} = \sum_{l=1}^{L} R_B^l U[\log_2(1+P_B\gamma_B(i)) - R_B^l] - \sum_{l=1}^{L-1} R_B^l U[\log_2(1+P_B\gamma_B(i)) - R_B^{l+1}], \quad (74)$$

where $U(x)$ is the step function. As a result, by differentiating $\mathcal{L}$ with respect to P_1 and P_B, then, setting the result to zero, we obtain (36) and (37), respectively.

Moreover, using (72) and defining $-\lambda_5(i)+\lambda_6(i) \triangleq -\beta(i)$, we can find the state-selection scheme as follows. The conditions which maximize (71), in the cases when U1 transmits with R_1^m and BS is silent, are

$$[\mu\max_{m}\{R_1^m O_1^m(i)\} - \zeta_1 P_1 - \beta(i) > 0] \text{ and } [(1-\mu)\max_{l}\{R_B^l O_B^l(i)\} - \zeta_B P_B - \beta(i) < 0]. \quad (75)$$

On the other hand, for maximizing (72) in the cases when the BS transmits with R_B^l and U1 is silent, are

$$[\mu\max_{m}\{R_1^m O_1^m(i)\} - \zeta_1 P_1 - \beta(i) < 0] \text{ and } [(1-\mu)\max_{l}\{R_B^l O_B^l(i)\} - \zeta_B P_B - \beta(i) > 0]. \quad (76)$$

In (75) and (76), we can substitute $\mu\max_{m}\{R_1^m O_1^m(i)\} - \zeta_1 P_1$ with $\Lambda_1(i)$ and $(1-\mu)\max_{l}\{R_B^l O_B^l(i)\} - \zeta_B P_B$ with $\Lambda_B(i)$, and thereby obtain the state-selection scheme. This completes the proof.

REFERENCES

[1] H. Holma and A. Toskala, *LTE for UMTS: Evolution to LTE-Advanced*. Wiley, 2011.

[2] S. Shakkottai and P. C. Karlsson, "Cross-layer design for wireless networks," *IEEE Communications Magazine*, vol. 41, pp. 74–80, 2003.

[3] N. Zorba and A. I. Perez-Neira, "Robust power allocation schemes for multibeam opportunistic transmission strategies under quality of service constraints," *IEEE Journal on Selected Areas in Communications*, vol. 26, no. 6, pp. 1025–1034, August 2008.

[4] E. Kartsakli, N. Zorba, L. Alonso, and C. V. Verikoukis, "A threshold-selective multiuser downlink mac scheme for 802.11n wireless networks," *IEEE Transactions on Wireless Communications*, vol. 10, no. 3, pp. 857–867, March 2011.

[5] M. J. Hossain, M. s. Alouini, and V. K. Bhargava, "Rate adaptive hierarchical modulation-assisted two-user opportunistic scheduling," *IEEE Transactions on Wireless Communications*, vol. 6, no. 6, pp. 2076–2085, June 2007.

[6] M. A. Haleem and R. Chandramouli, "Adaptive downlink scheduling and rate selection: a cross-layer design," *IEEE Journal on Selected Areas in Communications*, vol. 23, no. 6, pp. 1287–1297, June 2005.

[7] Q. Liu, S. Zhou, and G. B. Giannakis, "Cross-layer scheduling with prescribed qos guarantees in adaptive wireless networks," *IEEE Journal on Selected Areas in Communications*, vol. 23, no. 5, pp. 1056–1066, May 2005.

[8] H. Nam, Y. c. Ko, and M. s. Alouini, "Performance analysis of joint switched diversity and adaptive modulation," *IEEE Transactions on Wireless Communications*, vol. 7, no. 10, pp. 3780–3790, October 2008.

[9] S. N. Donthi and N. B. Mehta, "An accurate model for eesm and its application to analysis of cqi feedback schemes and scheduling in lte," *IEEE Transactions on Wireless Communications*, vol. 10, no. 10, pp. 3436–3448, October 2011.

[10] H. Kwon, S. Kim, and B. G. Lee, "Opportunistic multi-channel csma protocol for ofdma systems," *IEEE Transactions on Wireless Communications*, vol. 9, no. 5, pp. 1552–1557, May 2010.

[11] S. S. Nam, M. S. Alouini, H. C. Yang, and K. A. Qaraqe, "Threshold-based parallel multiuser scheduling," *IEEE Transactions on Wireless Communications*, vol. 8, no. 4, pp. 2150–2159, April 2009.

[12] M. Katoozian, K. Navaie, and H. Yanikomeroglu, "Utility-based adaptive radio resource allocation in ofdm wireless networks with traffic prioritization," *IEEE Transactions on Wireless Communications*, vol. 8, no. 1, pp. 66–71, Jan 2009.

[13] C. H. Chiang, W. Liao, T. Liu, I. K. Chan, and H. L. Chao, "Adaptive downlink and uplink channel split ratio determination for tcp-based best effort traffic in tdd-based wimax networks," *IEEE Journal on Selected Areas in Communications*, vol. 27, no. 2, pp. 182–190, February 2009.

[14] V. Hassel, D. Gesbert, M.-S. Alouini, and G. E. Oien, "A threshold-based channel state feedback algorithm for modern cellular systems," *IEEE Transactions on Wireless Communications*, vol. 6, no. 7, pp. 2422–2426, July 2007.

[15] Y. Yu and G. B. Giannakis, "Opportunistic medium access for wireless networking adapted to decentralized csi," *IEEE Transactions on Wireless Communications*, vol. 5, no. 6, pp. 1445–1455, June 2006.

[16] A. Sabharwal, P. Schniter, D. Guo, D. Bliss, S. Rangarajan, and R. Wichman, "In-Band Full-Duplex Wireless: Challenges and Opportunities," *IEEE J. Select. Areas Commun.*, vol. 32, pp. 1637–1652, Sep. 2014.

[17] D. Nguyen, L. N. Tran, P. Pirinen, and M. Latva-aho, "On the spectral efficiency of full-duplex small cell wireless systems," *IEEE Transactions on Wireless Communications*, vol. 13, no. 9, pp. 4896–4910, Sept 2014.

[18] S. Goyal, P. Liu, S. S. Panwar, R. A. Difazio, R. Yang, and E. Bala, "Full duplex cellular systems: will doubling interference prevent doubling capacity?" *IEEE Communications Magazine*, vol. 53, no. 5, pp. 121–127, May 2015.

[19] R. Lopez-Valcarce, E. Antonio-Rodriguez, C. Mosquera, and F. Perez-Gonzalez, "An adaptive feedback canceller for full-duplex relays based on spectrum shaping," *IEEE Journal on Selected Areas in Communications*, vol. 30, no. 8, pp. 1566–1577, September 2012.

[20] Y. Sun, D. W. K. Ng, J. Zhu, and R. Schober, "Multi-objective optimization for robust power efficient and secure full-duplex wireless communication systems," *IEEE Transactions on Wireless Communications*, vol. 15, no. 8, pp. 5511–5526, Aug 2016.

[21] D. Wen and G. Yu, "Time-division cellular networks with full-duplex base stations," *IEEE Communications Letters*, vol. 20, no. 2, pp. 392–395, Feb 2016.

[22] J. M. B. da Silva, G. Fodor, and C. Fischione, "Spectral efficient and fair user pairing for full-duplex communication in cellular networks," *IEEE Transactions on Wireless Communications*, vol. 15, no. 11, pp. 7578–7593, Nov 2016.

[23] B. Di, S. Bayat, L. Song, Y. Li, and Z. Han, "Joint user pairing, subchannel, and power allocation in full-duplex multi-user ofdma networks," *IEEE Transactions on Wireless Communications*, vol. 15, no. 12, pp. 8260–8272, Dec 2016.

[24] F. Boccardi, J. Andrews, H. Elshaer, M. Dohler, S. Parkvall, P. Popovski, and S. Singh, "Why to decouple the uplink and downlink in cellular networks and how to do it," *IEEE Commun. Magazine*, vol. 54, no. 3, pp. 110–117, Mar. 2016.

[25] S. Boyd and L. Vandenberghe, *Convex Optimization*. Cambridge University Press, 2004.

[26] J. Laneman, D. Tse, and G. Wornell, "Cooperative Diversity in Wireless Networks: Efficient Protocols and Outage Behavior," *IEEE Trans. Inf. Theory*, vol. 50, pp. 3062–3080, Dec. 2004.